

Salt-dependent intermolecular interactions of hyaluronan molecules mediate the formation of temporary duplex structures

Citation

KOLAŘÍKOVÁ, Alena, Eva KUTÁLKOVÁ, Václav BUŠ, Roman WITASEK, Josef HRNČIŘÍK, and Marek INGR. Salt-dependent intermolecular interactions of hyaluronan molecules mediate the formation of temporary duplex structures. *Carbohydrate Polymers* [online]. vol. 286, Elsevier, 2022, [cit. 2023-04-26]. ISSN 0144-8617. Available at <https://www.sciencedirect.com/science/article/pii/S0144861722001928>

DOI

<https://doi.org/10.1016/j.carbpol.2022.119288>

Permanent link

<https://publikace.k.utb.cz/handle/10563/1010880>

This document is the Accepted Manuscript version of the article that can be shared via institutional repository.

Salt-dependent intermolecular interactions of hyaluronan molecules mediate the formation of temporary duplex structures

Alena Kolanková^a, Eva Kutalková^a, Vaclav Bus^a, Roman Witasek^a, Josef Hrnčík^a, Marek Ingr^{a,b,*}

^a Tomas Bata University in Zlín, Faculty of Technology, Department of Physics and Materials Engineering, Nám. T.G. Masaryka 5555, 76001 Zlín, Czech Republic

^b Charles University, Faculty of Science, Department of Biochemistry, Hlavova 8/2030, 12843 Praha 2, Czech Republic

* Corresponding author at: Tomas Bata University in Zlín, Faculty of Technology, Department of Physics and Materials Engineering, Nam. T.G. Masaryka 5555, 76001 Zlín, Czech Republic. E-mail address: ingr@utb.cz (M. Ingr).

ABSTRACT

Hyaluronic acid (HA) is a natural polysaccharide present in the connective tissues of vertebrates, often used in the cosmetics and pharmaceutical industries. HA is a strongly hydrophilic macromolecule forming highly swollen random coils in aqueous solutions. Although some authors reported the secondary and tertiary structures of HA chain, others brought convincing evidence contradicting this hypothesis. This study aims at investigation of the stability and dynamics of the temporary duplex HA structures at different NaCl concentrations by molecular-dynamics (MD) simulations. The tendency to duplex formation grows with NaCl concentration reaching its maximum at 0.6 M. This profile is a result of two counteracting NaCl-concentration dependent phenomena, the growing electrostatic-repulsion screening on one side and the disturbance of hydrogen-bonds formation on the other side. Although the weak intermolecular attraction cannot lead to long-lived secondary and tertiary structures, it may influence the properties of large HA macromolecules and concentrated HA solutions.

Keywords: Hyaluronan, Duplex, Hydrogen bond, Molecular dynamics, Fixed chains

1. Introduction

Hyaluronic acid (hyaluronan, HA) is a highly hydrophilic natural polysaccharide consisting of the alternating monosaccharide units of glucuronic acid (GCU) and N-acetylglucosamine (NAG) of the formula $[(4)\text{-}\beta\text{-D-GlcpA-(1}\rightarrow\text{3)-p-D-GlcpNAc-(1}\rightarrow\text{)]}_n$. In aqueous solutions the HA macromolecule adopts a disordered conformation and forms a highly swollen random coil that has been characterized both experimentally (Fouissac, Milas, Rinaudo, & Borsali, 1992; Hayashi, Tsutsumi, Naka-jima, Norisuye, & Teramoto, 1995; Mendichi, Soltes, & Giacometti Schieroni, 2003) and theoretically (Holmbeck, Petillo, & Lerner, 1994; Ingr, Kutálková, & Hrnčík, 2017) in the molecular-weight range of $10^3 - 10^7$ Da. However, under specific conditions secondary and tertiary structures of HA chains were observed. This was the case especially in crystals (Arnott, Mitra, & Raghunathan, 1983; Dea et al., 1973; Sheehan, Gardner, & Atkins, 1977) where double helices of 1-2 MDa HA were found. Similar structures were observed also in mixed solvents of water and ethanol by means of circular dichroism on both oligosaccharides up to 20 kDa and polymer of about 200 kDa (Staskus & Johnson, 1988a, b). Although in aqueous solutions stable regular double-helical structures were not observed, ¹³C NMR studies identified intermolecular interactions that indicate the formation of reversible tertiary structures in a concentrated solution (10 mg/ml) of high molecular weight ($\sim 10^6$ Da) HA even in this

environment (**Scott & Heatley, 1999, 2002**). An influence of shear flow on the formation of these structures was shown by rheo-NMR spectroscopy (**Fischer, Callaghan, Heatley, & Scott, 2002**) on HA samples of equal concentration and molecular weight. These findings were, however, contradicted by confocal-FRAP (fluorescence recovery after photobleaching) assay on 0.5-1 MDa HA (**Gribbon, Heng, & Hardingham, 2000**) and later also by ¹⁵N NMR study on HA oligosaccharides up to 40 monosaccharide units showing the low population of amide hydrogen bond that is incompatible with formation of tertiary structures (**Blundell, DeAngelis, & Almond, 2006**). These findings were further supported by Raman and Raman optical activity (ROA) spectroscopies on HA polymer of 500 monosaccharide units (**Yaffe, Almond, & Blanch, 2010**). In spite of that, tertiary structures were later considered as the cause of the break in the temperature dependence of the behavior of highly concentrated solutions of 1 MDa HA (**Matteini et al., 2009**). Recently, a direct observation of hydrogen bonds between the carboxyl and amide groups of different HA chains (samples of 1.5-1.8 MDa and 150 kDa) by two-dimensional infrared spectroscopy (2D-IR) spectroscopy was reported (**Giubertoni, Burla, et al., 2019**) at low pH where the supramolecular-structure formation is supported by the protonation, and thus discharging, of carboxyl groups. Intramolecular amide-carboxyl HA bonds were detected by the same method on similar HA samples in a wider pH range (**Giubertoni, Koenderink, et al., 2019**).

Molecular-dynamics (MD) simulations are an attractive instrument of the study of intermolecular interactions on an atomistic level. Several studies used this approach to investigate the structure and dynamics of HA chains, especially its rigidity, dihedral angles of the glycosidic chains, intramolecular hydrogen bonds and other parameters (**Almond, Deangelis, & Blundell, 2006; Donati, Magnani, Bonechi, Barbucci, & Rossi, 2001; Furlan, La Penna, Perico, & Cesaro, 2005; Holmbeck et al., 1994; Samantray, Olubiyi, & Strodel, 2021**). More recently MD studies of HA modified by aliphatic sidechains (**Payne, Svechkarev, Kyrychenko, & Mohs, 2018**) and HA in non-aqueous environment were carried out (**Betdowski, Mazurkiewicz, Topoliński, & Małek, 2019; Siódmiak et al., 2017; Smith, Ziolek, Gazzarrini, Owen, & Lorenz, 2019**). However, interactions of two HA chains, to our knowledge, have not been studied by MD yet.

Our recent MD studies of HA in solutions of electrolytes describing the structure (**Ingr et al., 2017**) and dynamics (**Kutalkova, Hrnčink, Witasek, & Ingr, 2020**) of its random coils show a good agreement with the experimental values of the radius of gyration and its dependence on NaCl concentration. In both these studies just one HA molecule was simulated, therefore the interactions of the distant parts of HA chains were neglected. However, these interactions may play a non-negligible role in highly concentrated HA solutions, in the centers of high-molecular-weight random coils or in non-aqueous solutions. Therefore, the present work is based on molecular-dynamics simulations of a couple of HA chains in order to investigate their mutual interactions in different conditions, i.e. NaCl concentrations and temperatures. Comparing the results with published experimental observations, our aim is to show that the presence of dissolved ions causes the formation of temporary duplex structures of two HA chains that may influence the macroscopic behavior of hyaluronan solutions.

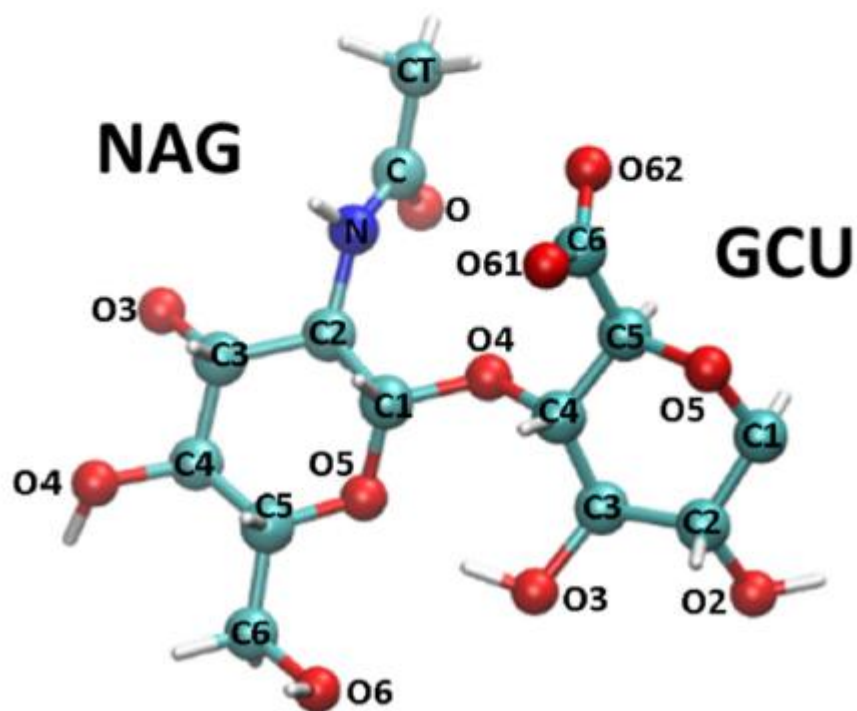
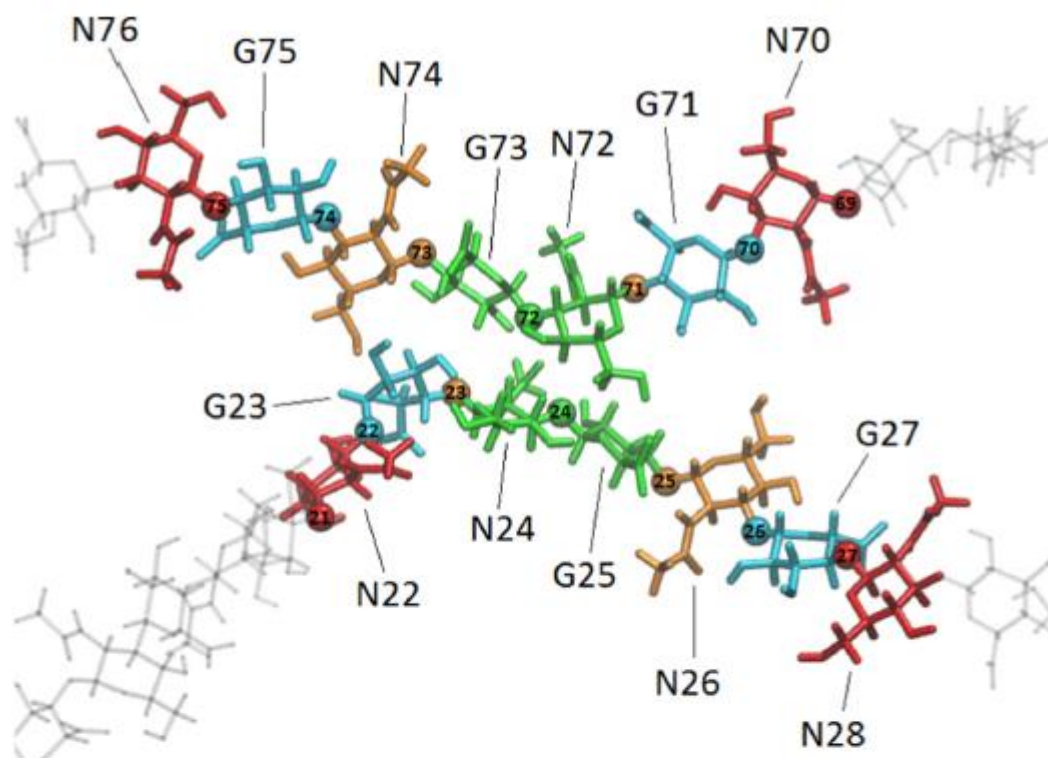


Fig. 1. Top: a scheme of the subsequent exclusions of residues from the fixed HA oligosaccharides in the calculations of the number of intermolecular hydrogen bonds and the mean distances. In case of hydrogen bonds counting, the fixed residues (24, 25 on one chain, 72, 73 on the other chain) plotted in green are excluded first followed by 26 and 74 (ocher), then 23, 27 and 71, 75 (blue) and finally 22, 28 and 70, 76 (red). In the mean-distance calculations the glycosidic oxygens are being subsequently excluded according to the same colour scheme. Bottom: Definitions of acronyms of atoms constituting the HA monomer. If necessary, atoms of GCU are labeled by G and of NAG by N (e.g. oxygen O3 of GCU is denoted as G O3, etc.). (For interpretation of the references to color in this figure legend, the reader is referred to the web version of this article.)

2. Methods

Two antiparallel HA chains, each of 48 monosaccharide units with all carboxyl groups dissociated, were simulated in 1 M, 0.6 M, 0.2 M and 0 M NaCl (plus neutralizing Na⁺ cations) solution at two temperatures, 275 K and 310 K. The initial conformation, identical for both the chains, was taken from the equilibrium phase of the single-chain simulation in 0 M NaCl done previously (**Ingr et al., 2017**). The two chains were put close to one another and solvated by a water box of approx. (160 x 120 x 180) Å³ with the explicit TIP3P solvent model, periodic boundary conditions in the isobaric-isothermal (NPT) ensemble were applied. Simulations were performed using the NAMD version 2.10 (**Phillips et al., 2005**) software packages with CHARMM36 (**Guvench et al., 2009**) carbohydrate topologies and force field parameters. A timestep of 1 fs for bonded and 2 fs for non-bonded interactions and 10 Å cutoff of nonbonded interactions were used. Full electrostatic calculations were performed every sixth fs using the Particle Mesh Ewald method (PME). Prior to each MD simulation the energy of systems was minimized for 180 fs. Subsequent simulations were carried out at the constant pressure of 1 atm and a selected temperature. The pressure was controlled using the Langevin piston Nose-Hoover method and the temperature was controlled using Langevin dynamics. Coordinates of all atoms were stored every 1800 fs and data were processed in VMD 1.9.3. (**Humphrey, Dalke, & Schulten, 1996**). Two variants of the simulations were carried out. In the first one the chains were free and no constraint was applied to their motion, while in the second one specific atoms of the two middle residues of each chain (C of NAG24, C6 of GCU25, C6 of NAG72 and C2 of GCU73, see **Fig. 1** for the atom acronyms) were kept in fixed positions.

Simulations of couples of HA chains in an artificial environment with the HA-solvent electrostatics interactions switched off were performed using the GROMACS version 5.1.1 (**Van Der Spoel et al., 2005**) software packages with GROMOS 56A(CARBO) (**Hansen & Hunenberger, 2011**) carbohydrate topologies and force field parameters. (The calculations were adapted from our different project in which different software is used.) Two parallel or antiparallel HA chains with carboxyl groups either fully dissociated or fully protonated, each of 12 monosaccharide units, were simulated in water (containing eventual neutralizing Na⁺ ions) at 275 K. Oligosaccharide molecules were placed in the center of a cubic box (120 x 120 x 120) Å³. The simulation box was filled with SPC/E water-model molecules. Periodic boundary conditions were applied. Initially, the steepest descents integrator was used to obtain the energy-minimized structures of the model system. Following this, the whole system was equilibrated under an isothermal-isochoric NVT ensemble. Finally, an all-atom MD simulation followed using Langevin dynamics with a timestep of 2 fs. Details of all the simulated systems are given in Table S1.

As a characteristic of the mutual interaction of two HA chains the mean distance of the chains was defined. It is equal to the distance of two parallel straight non-overlapping HA chains showing equal interchain electrostatic energy of the glycosidic oxygen atoms as the really simulated HA chains. For details of its evaluation, carried out using the MDAnalysis toolkit (**Michaud-Agrawal, Denning, Woolf, & Beckstein, 2011**), see section SM1 of Supplementary data.

Number of hydrogen bonds was evaluated using the VMD 1.9.3 program package. The donor-H-acceptor group of atoms was considered as a hydrogen bond if the distance between the donor and acceptor was up to 3 Å and the deflection from the straight angle on the hydrogen atom up to 20°. Analysis shown in Fig. S2 indicates the reasonability of this criterion.

In case of the fixed HA chains both the number of intermolecular hydrogen bonds and the mean distances were evaluated not only for the whole chains, but also for the chains from which residues of the fixed region were excluded. A series of such evaluations was carried out with subsequent

exclusions of residues according to the scheme in **Fig. 1**. Acronyms of individual atoms used throughout the text are defined in **Fig. 1**, too.

3. Results

3.1. Duplexes of HA are formed when the electrostatic interaction HA-solvent is switched off

Several research groups showed the ability of HA to form doublehelix structures in special cases. In aqueous solutions, however, their existence is disabled by the high hydrophilicity of HA resulting in dissolution of individual HA molecules. On the other hand, single HA chains adopt an irregular helical conformation (**Almond et al., 2006; Ingr et al., 2017**) indicating their inherent tendency to constitute this shape. To investigate the ability of the HA chains to form double helices, we carried out short 10 ns simulations with couples of HA oligosaccharides of 12 monosaccharide units, in both parallel and anti-parallel orientations, in an artificial environment in which the HA-solvent electrostatic interaction is turned off. The choice of the short oligosaccharides is practical because of their ability to assume the conformation enforced by the mutual interactions quickly. On the other hand, they form the duplex only when the interaction is sufficiently strong, otherwise they tend to fast separation.

The HA chains thus interact with solvent only by the dispersion forces represented by Lennard-Jones potentials and their behavior resembles strongly hydrophobic bodies. The artificial environment thus supports both the hydrogen bonding and hydrophobic interaction making thus the attraction of the chains highly favorable. The simulations show that HA with the dissociated carboxylic (hereinafter called carboxylate) groups is not able to form duplexes of any kind and has a direct tendency to the chain separation due to the strong electrostatic repulsion. On the contrary, a neutral HA with completely protonated carboxylic groups forms duplexes in both the parallel and anti-parallel orientations (**Fig. 2**). Thus, the artificially hydrophobized neutral HA chains show a well pronounced tendency to form double-helices, although not absolutely regular, indicating the structural favorableness of this conformation. On the other hand, neither the neutral oligosaccharides were observed to form stable double helices in simulations of realistic aqueous solvents since their strong solvation protects them from mutual interactions.

Even though no water competes with the HA groups for the hydrogen bonding capacities, the number of intermolecular hydrogen bonds is rather low compared to the intramolecular ones, below 5% for both the orientations. Therefore, in agreement with the previous findings such stable duplexes can be formed only in a non-polar environment or crystalline phase and cannot be expected in water where the hydrophobic interaction vanishes while no other stabilizing interaction occurs.

3.2. Total interaction between the HA chains depends on NaCl concentration

MD simulations of a couple of HA oligosaccharide chains of 48 monosaccharide units each were carried out at four different NaCl concentrations and two different temperatures. Initially, the chains were put next to one another in either parallel or anti-parallel orientation so that the distance between their closest atoms is below the range of direct interatomic interaction, i.e. 10 Å. As the frequency of interactions was apparently higher for the anti-parallel arrangement, we continued the calculations only with this orientation. All the simulations described below started from an equal conformation. At first the two chains were evolved in the simulation box without any further constraints. Although the chains did not show any tendency to form stable tertiary structures, interactions between them were observed causing at least temporary stabilization of the chains close to each other.

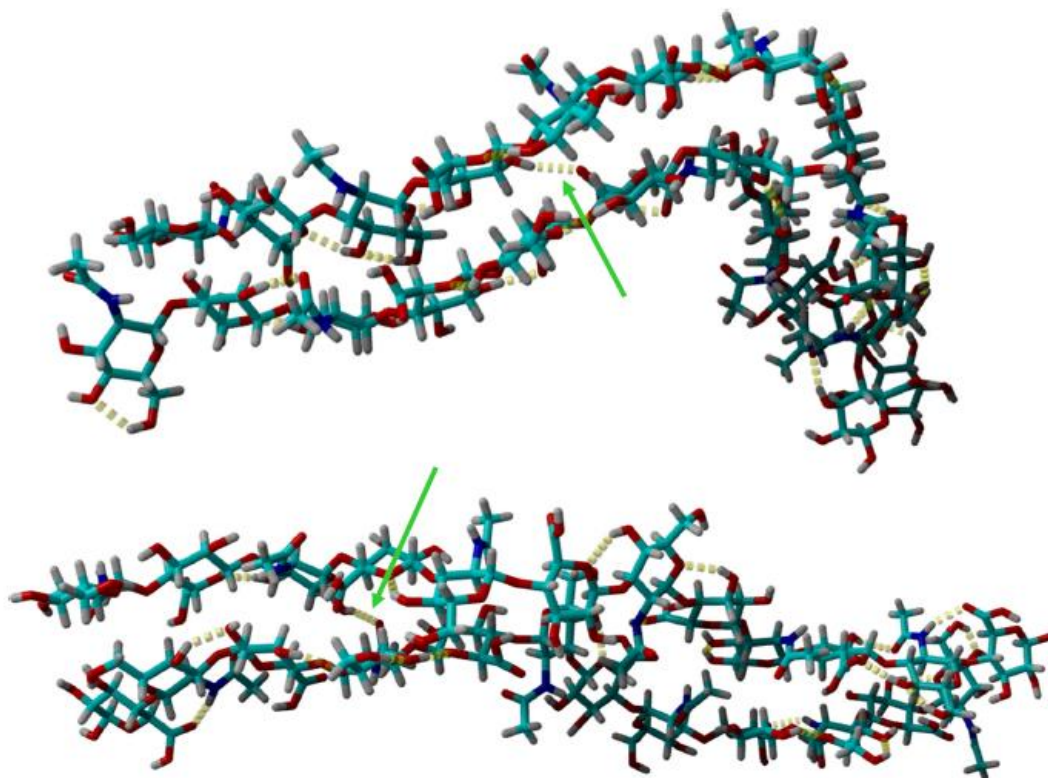


Fig. 2. Double helices of HA chains formed in an artificial solvent non-interacting electrostatically with HA in parallel (top) and anti-parallel (bottom) orientations. Hydrogen bonds are indicated by the yellow dashed lines, green arrows indicate intermolecular hydrogen bonds. The graphics was made using YASARA program (Krieger & Vriend, 2014). (For interpretation of the references to colour in this figure legend, the reader is referred to the web version of this article.)

As a measure of the duplex stability a mean distance of the two chains was chosen (see section SM1 for the definition). At the beginning of every simulation this distance was approx. 15 Å and its increase was observed during the course of the simulation (Fig. S3). The rate of the distance increase strongly depending on the NaCl concentration in the solution. While in pure water the chains separate immediately, the increasing NaCl concentration makes this process much slower indicating its stabilization effect reaching its maximum at 0.6 M NaCl. This is also documented by the value of the mean intermolecular distance averaged over the whole simulation period (Fig. S4) which shows an obvious minimum at this concentration. However, the simulated HA-chain couples cannot be considered as equilibrium structures, the calculations should be rather seen as a dynamic experiment revealing the decay rate of the temporary duplexes.

To reach the equilibria between the duplexed and free HA chains, additional simulations were carried out in all the considered environments with the two middle residues of each chains held in fixed positions keeping the central parts of the chains in a close contact. To avoid the influence of the artificially fixed region of the chains, the mean distance between them was evaluated in several variants differing in the number of residues around the fixation point excluded from the calculation (see Fig. 1). The result is shown in Figs. 3 and S5 (time dependencies). At both the temperatures the shortest mean distance occurs in 0.6 M NaCl indicating the strongest intermolecular interaction in this environment. On the contrary, the weakest interaction is observed in pure water for both the temperatures. At 275 K the mean distance is generally shorter than at 310 K showing the temperature destabilization of the duplex structures.

Furthermore, the points depicting individual variants of the calculation are more packed at the shortest mean distances, especially at 275 K, indicating that the interaction between the two chains is not limited only to the close surrounding of the fixation point but is spread along the whole length of the chains. At 1 M NaCl the mean distance grows in comparison with 0.6 M at both temperatures, but this increase is considerably higher at the higher temperature. This dependence apparently agrees with the analogous trend for the non-fixed chains (Fig. S4) confirming the influence of NaCl concentration on the stability of HA duplexes in aqueous solutions.

3.3. Total charge of HA chains moderates HA-HA interactions

To explain the NaCl-concentration dependent profile of the intermolecular interactions, we calculated the total charges of the HA molecules together with the Na⁺ and Cl⁻ ions occurring within a set of distances from HA ranging from 3 to 7 Å. As the ion distribution equilibrates quickly, the calculations were done on the non-fixed chains within 20 ns simulation intervals in which the chains were separated sufficiently.

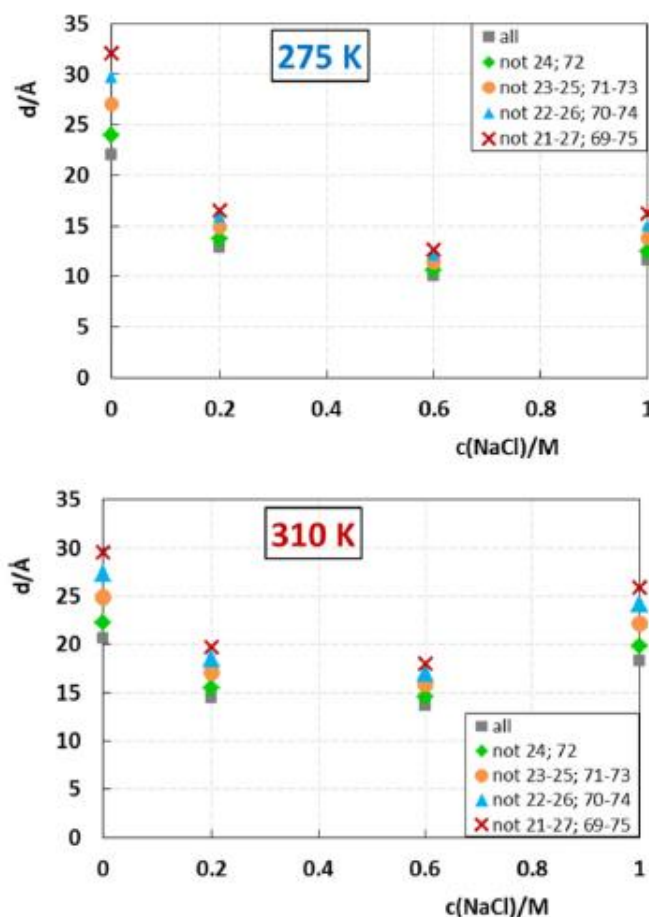


Fig. 3. Mean distance between the fixed HA chains as a function of NaCl concentration for two temperatures. Different symbols correspond with different versions of excluding the residues surrounding the point of fixation. Standard deviations of the mean are smaller than the size of the symbols.

The monotonous decrease of the total negative charge with the growing NaCl concentration can be observed within all the selected distances (**Fig. 4**). Contributions of individual ions to this effect can be seen in Fig. S6. Therefore, the approach of the chains in pure water is prevented by the electrostatic repulsion, but with the increasing NaCl concentration the repulsion decreases rapidly allowing the intermolecular interaction already at 0.2 M. Hence, the intermolecular interactions are enabled especially by screening the molecular charge by the dissolved ions. Contrary to its rather weak influence on the HA random-coil size discussed by us previously (**Ingr et al., 2017**), its effect on the intermolecular interactions is obviously stronger due to the necessary approach of the chains to the distance of hydrogen-bond formation.

3.4. Number of intermolecular hydrogen bonds correlates with the mean distance of the chains

The total number of the interchain hydrogen bonds as a function of time was evaluated for all the systems of the fixed chains. These calculations were also carried out in several variants excluding subsequently individual residues of the fixed region, in a direct analogy to the meandistance evaluations. As expected, the total number of interchain hydrogen bonds decreases with the subsequent residue exclusions and the differences between them are practically independent on both NaCl concentration and temperature, reaching a stabilized value between 5 and 7 excluded residues on each chain (**Fig. 5**). This number thus corresponds with the hydrogen bonds within the regions of the chains distant from the fixation point.

The number of hydrogen bonds between the chains is relatively small, in average less than 1 per simulation frame, which is in agreement with the generally accepted inability of HA to form stable tertiary structures. In spite of that, a clear dependence of the number of hydrogen bonds on the salt concentration was observed. Considering only the outer region of the chains (fixed part excluded), the trend of the number of hydrogen bonds is perfectly reciprocal to the trend of the mean distance of the chains (**Fig. 3**), regarding both the NaCl-concentration and temperature dependences.

A more detailed documentation of this concentration dependence is shown in **Fig. 6** where the time dependence of the number of hydrogen bonds of individual residues is plotted. At every NaCl concentration the numbers are high for the residues closely surrounding the residues 25 and 71 containing the point of fixation. However, the plots differ considerably for the more distant residues. The highest frequency of non-zero values can be seen for 0.6 M NaCl, somewhat less for 0.2 M NaCl and even less for 1 M NaCl, in accord with **Fig. 5**. It can also be seen that even the most distant residues are involved in the interactions and that the interaction positions are changing during the simulation. Analogous analysis for the non-fixed chains (Fig. S7) gives similar results, but the number of hydrogen bond vanishes in time along with the continuous chain separation.

3.5. Hydrogen bonds between the individual functional groups of HA

The involvement of individual functional groups in the formation of intermolecular hydrogen bonds was analyzed on the fixed-chains couples excluding residues 22-28 and 70-76 of the fixed region. Neglecting the terminal hydroxyl groups on C3 of NAG and C1 of GCU, there are five H-bond donor groups in HA molecule, i.e. the hydroxyl groups on C2 and C3 of GCU and on C4 and C6 of NAG as well as the nitrogen atom of the amide group of NAG. At 0 M NaCl almost no hydrogen bonds are constituted at any temperature, the same is valid for 1 M NaCl at 310 K (compare **Fig. 5**). In other cases, the most frequent donor groups are the C2 and C3 hydroxyls of GCU (**Fig. 7**). The other groups play the

role mainly at low NaCl concentrations. Although all oxygen and nitrogen atoms are potential hydrogen-bond acceptors, significant contributions are provided only by the oxygens of the carboxylate group, C2 and C3 hydroxyl-group oxygens of GCU, oxygen of acetyl group, and C6 hydroxyl groups of NAG (Fig 7). As can be seen in Fig. 8, the most frequent donor-acceptor couple consists of the GCU hydroxyls on C2 or C3 as a donor and the carboxylate group as an acceptor (for example of the structures see Fig. S8).

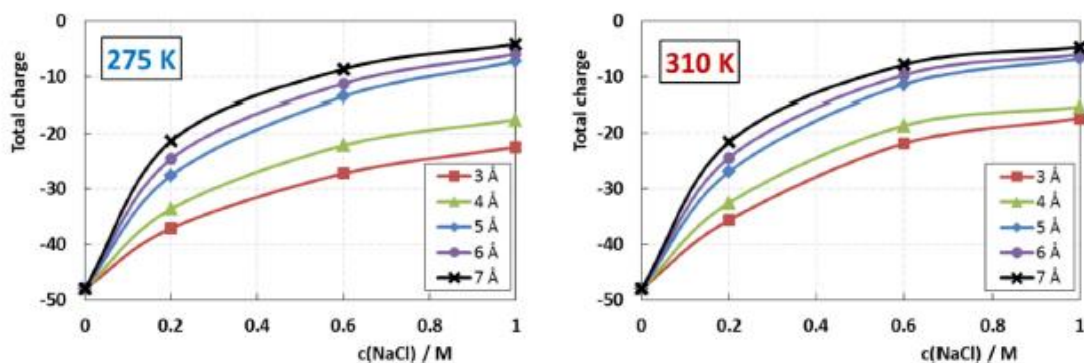


Fig. 4. Total charge of HA chains including their local surroundings for two temperatures. It includes the charge of HA carboxylate groups plus the Na^+ and Cl^- ions within certain distances from 3 to 7 Å.

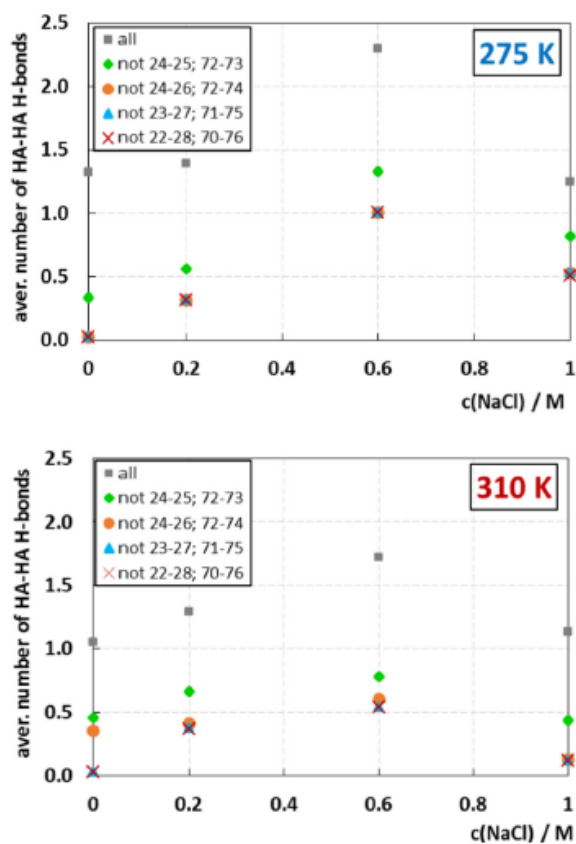


Fig. 5. Number of intermolecular hydrogen bonds between the fixed HA chains as a function of NaCl concentration at two different temperatures. Different symbols correspond with different versions of excluding the residues surrounding the area of fixation. Standard deviations of the mean are smaller than the size of the symbols.

The role of carboxylate as an acceptor is supported especially by its negative charge as well as by the two oxygen atoms able to participate in the hydrogen bond. On the donor side, the two vicinal hydroxyls attract the acceptor by the doubled positive partial charge and they also double the probability of catching the partner. As we showed previously (**Kutálková et al., 2020**), the surroundings of these two groups behaves as a strongly hydrophilic region where the solvating water molecules are strictly organized by hydrogen bonding to these hydroxyls. Therefore, a strong acceptor as carboxylate can easily overtake the role of water and get hydrogen-bonded to them. However, when this kind of a hydrogen bond is formed, the acceptor carboxylate group gets relatively close to the carboxylate on the donor GCU residue which destabilizes the bond by electrostatic repulsion. Hence, it is preferred at higher NaCl concentrations where the carboxylate charge is screened by Na⁺ cations. At lower NaCl concentration other hydrogen bonds, that allow larger separation of the carboxylate charges, become more frequent (**Fig. 8**). They involve either the NAG groups or the GCU O2 and O3 hydroxyls also as acceptors (**Fig. S8**). While at 310 K the described high-low NaCl concentration change in hydrogen bonding is apparent between 0.2 and 0.6 M NaCl, at 275 K the ratios of different donor and acceptor groups at 0.6 M still have the low-concentration features, in spite of the higher total number of hydrogen bonds. This can be attributed to the anomalously low binding of Na⁺ cations by the carboxylate groups at 0.6 M NaCl reported by us previously (**Kutálková et al., 2020**).

3.6. Water and salt bridges between the HA chain

In addition to hydrogen bonds, the frequencies of water bridges (water molecules hydrogen-bonded to both the HA chains in the same frame) and salt bridges (Na⁺ cations occurring within 3 Å distance from each of the chains) were evaluated for the fixed couples of HA chains with the excluded region of fixation (in its maximum version according to **Fig. 5**). Both these quantities are generally lower than the number of interchain hydrogen bonds but together they provide a comparable contribution to the number of HA-HA interactions. Their dependence on NaCl concentration is similar to that of the interchain hydrogen bonds (**Fig. S9**). Hence, a non-negligible stabilization effect of the temporary HA duplex structures can be provided by these two kinds of interactions. For more details see the caption of **Fig. S9**.

3.7. Interacting HA chains keep the conformation of free molecules

Previously we showed (**Kutálková et al., 2020**) that the individual HA residues may undergo flips from their equilibrium orientation within the chain. The frequency of the flips is NaCl-concentration dependent and their occurrence has a substantial influence on the chain conformation. Therefore, we analyzed the frequency of the flips in the interacting chains to find out whether they play a role also in the intermolecular interactions. However, it seems that the number of flipped residues in the interacting chains does not differ from that of the free chains — compare the data for the distribution of values of the most flexible dihedral 14_2 from (**Kutálková et al., 2020**) with **Fig. S10** (containing also the definition of dihedrals). Moreover, although some flipped residues involved in the intermolecular hydrogen bonding were found, it does not seem to be a typical case and the flips are not correlated with intermolecular interactions. This further confirms the weakness of the intermolecular interactions that are incapable of enforcing the change of the molecular conformation.

4. Discussion

Interactions between two HA chains in aqueous solutions are generally weak due to the strong solvation of the hydrophilic molecules and, in addition, are hindered by the electrostatic repulsion of negatively charged carboxylate groups. In spite of this double-helical structures may be formed in case that the molecular negative charge is neutralized, i.e. in acidic conditions, and if the HA-solvent interactions are very weak. Such conditions may, in principle, occur in non-aqueous solvents (**Staskus and Johnson, 1988a, b**) or in crystals (**Arnott et al., 1983; Dea et al., 1973; Sheehan et al., 1977**) where structures of this kind were really observed. On the contrary, in aqueous environment the HA-HA interactions are weak and may take place only in salt solutions in which the electrostatic-repulsion screening allows the intermolecular hydrogen bonding. Even then the formation of tertiary structures in aqueous solutions, presumed by several authors, is thermodynamically unfavorable, as shown by other experimental findings. Nevertheless, interactions between the two chains leading to the formation of shortlived hydrogen bonded structures seem to be evident. Their strength grows with NaCl concentration up to approx. 0.6 M but above this value it continuously decreases. This trend is likely a result of two counteracting phenomena changing along with the increasing NaCl concentration — the decreasing negative charge of HA molecules including their solvation shells (see **Section 3.3.**) on one hand and the decreasing ability of hydrogen bonding on the other hand. The latter phenomenon, described in our previous work (**Kutálková et al., 2020**) (data from **Fig. 5** thereof are reproduced in Fig. S11), originates from the screening of the electrostatic attraction of the hydrogen atoms and their electronegative hydrogen-bonding partners (O or N) by the ions, especially Na⁺ cations, dissolved in the environment. While the hydrogen-bonding ability decreases rather moderately and constantly throughout the NaCl concentration range, the charge changes rapidly in the lower-concentration region becoming thus the leading contribution there. Above 0.6 M NaCl, however, the charge change is rather low and the hydrogen-bonding decrease becomes the dominant influence. The slight temperature-dependent shift of the maximum of the interaction intensity may be attributed to somewhat steeper charge decrease (in absolute value) at the high-concentration region (0.6-1.0 M) at 275 K that compensates better the hydrogen-bonding weakening compared to a very shallow profile at 310 K.

The NaCl-concentration dependence of the interaction intensity, and especially its maximum at about 0.6 M NaCl, indicate that HA may undergo salting-out and salting-in effects not only in NaCl, but also in different salts. As the interaction between the HA chains is weak, these phenomena can be expected only at higher HA concentrations or in solutions of large HA macromolecules being highly concentrated in the centers of their random coils. Possible occurrence of interactions between different HA chains was originally refuted by (**Gribbon et al., 2000**) at HA concentration below 10 mg/ml. A similar conclusion was reached by the NMR study of (**Blundell et al., 2006**) who worked at a similar concentration range. The absence of tertiary structures of HA was further reported by the combined Raman and ROA study (**Yaffe et al., 2010**) at HA concentration of 10 mg/ml. Considering the weakness of the intermolecular interactions observed in our simulations, a plausible explanation of these results is that the used combination of HA concentration and the ionic strength was not sufficient for an observable response of HA-HA interactions. The latter study, in addition, was carried out in a salt-free solution in which the interchain interactions are not favored. The results thus exclude the HA-HA interactions at certain conditions, but not necessarily in general. Although not much experimental evidence describing the behavior of HA in higher NaCl concentrations is available, several publications bring some data supporting our conclusions. **Mendichi et al. (2003)** showed that the intrinsic viscosity $[\eta]$ scales with an exponent decreasing along with the increasing molecular weight.

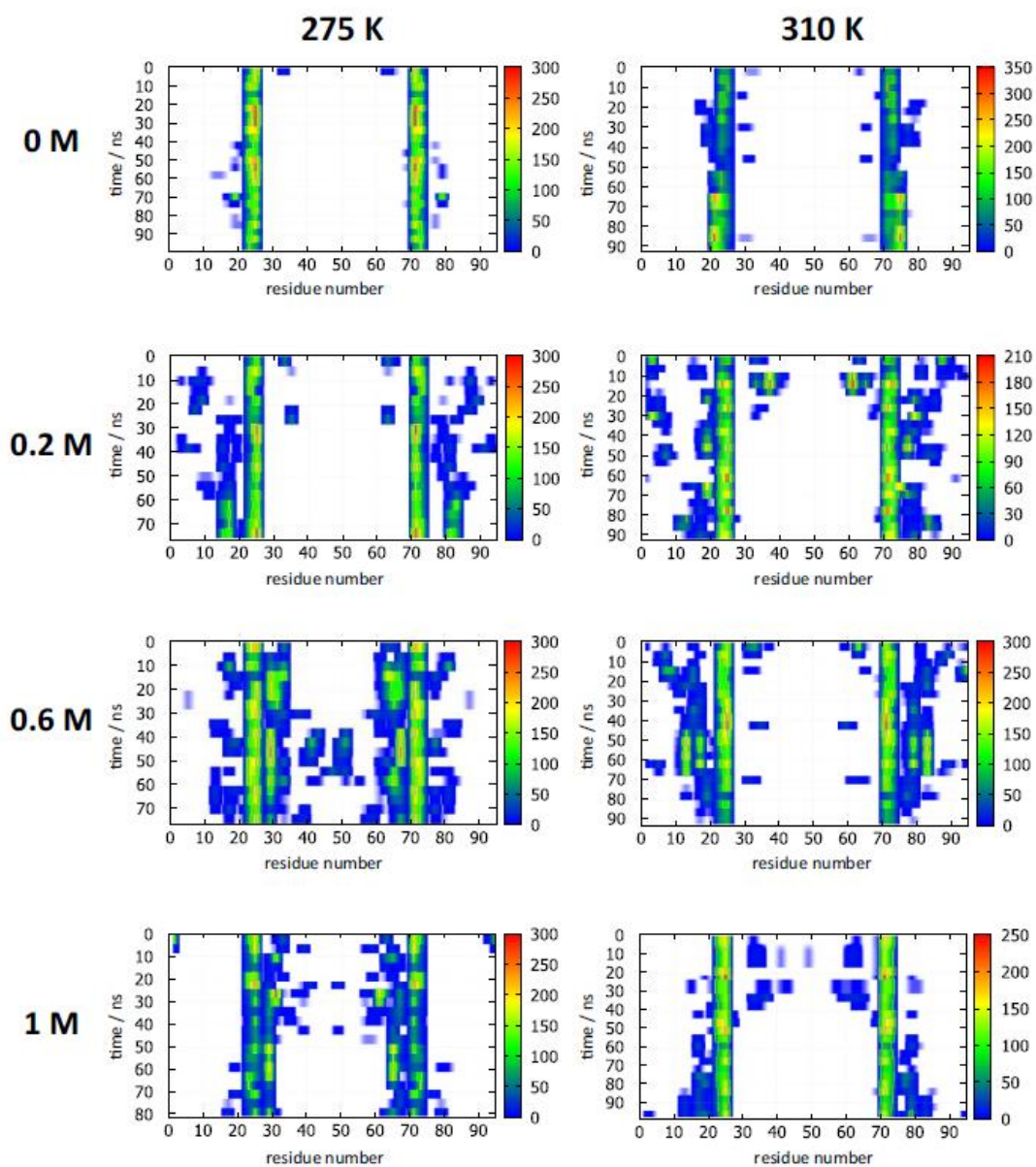


Fig. 6. Time dependence of the number of interchain hydrogen bonds of the fixed HA chains. The x-axis represents the residue number, 1-48 corresponds with the first and 49-96 to the second chain. The different colors show the different average numbers of hydrogen bonds for the given residue in a given time point.

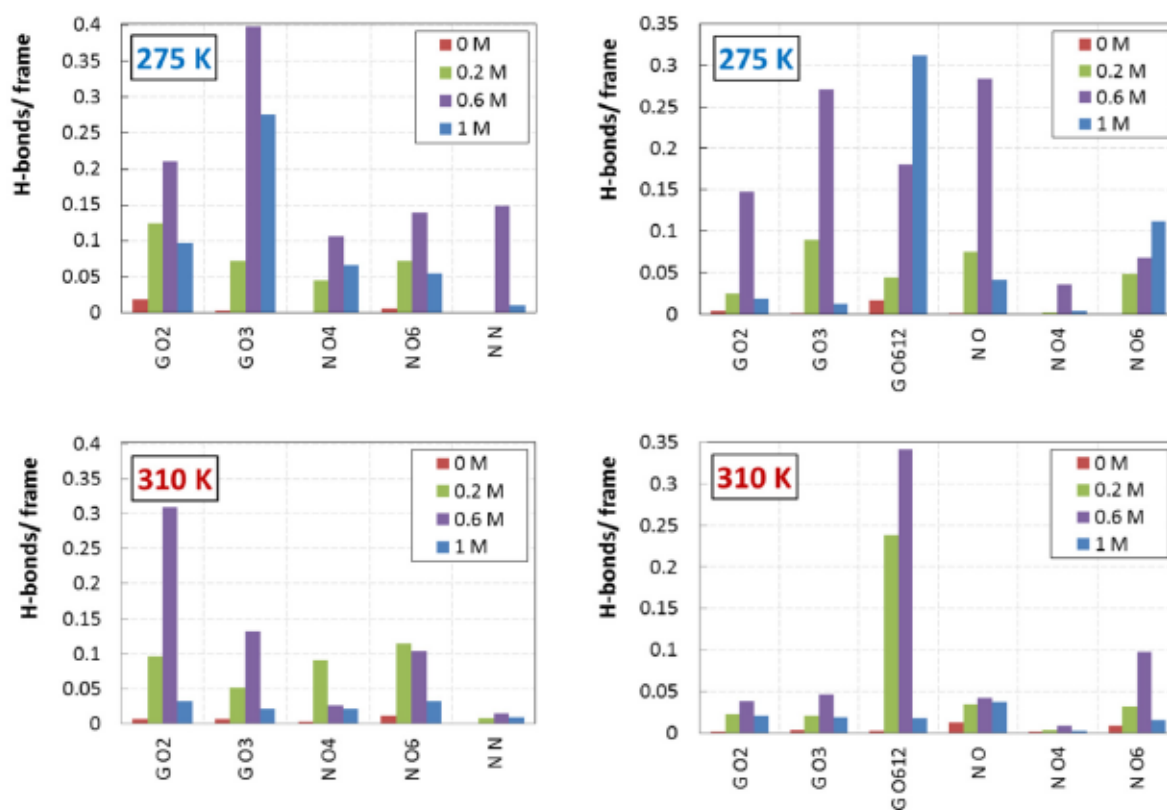


Fig. 7. Cumulative numbers of intermolecular hydrogen bonds for individual donor (left panels) and acceptor (right panels) groups for two temperatures and four NaCl concentrations. G O612 denotes the sum for G O61 and G O62.

The authors explain it by the change from a free-draining to non-free-draining random coil. Considering the low average density of the coils, it seems likely that this transition is caused by more frequent occurrence of the intramolecular interactions in the centers of the heavy random coils where the total HA concentration is higher. In even more concentrated solutions the interchain interactions seem to influence the dependence of viscosity on HA concentration (Yu, Zhang, Luan, Zhang, & Zhang, 2014). In the salt-free solution the viscosity is higher compared to the solution containing 0.15 M NaCl for low HA concentrations, but when HA concentration is growing, both the viscosities are getting closer and, finally, the trends get reversed at about 20 mg/ml. The behavior at low HA concentration with well separated molecules is clearly given by the larger random coils in the salt-free solution, a consequence of a higher chain rigidity in this environment, consistently with experimental results (Hayashi et al., 1995; Mendichi et al., 2003) as well as our recent model of an isolated random coil (Ingr et al., 2017). On the contrary, at the high HA concentrations the macromolecules get entangled which increases the viscosity in the salt-containing solutions due to the formation of intermolecular interactions, and thus intermolecular sticker points in accord with the sticky reptation model (Leibler, Rubinstein, & Colby, 1991). Applying the Cox-Merz rule (Cox & Merz, 1958), the same authors also show a remarkable increase of the intermolecular interactions at 20 mg/ml along with the growth of the molecular weight of HA molecules. Hence, coherently with our simulations that study shows the probable growth of the interchain interactions with NaCl concentration up to 0.15 M. Highly concentrated HA solutions reaching 100 mg/ml show a breakpoint on the trend of the viscosity decrease along with the temperature growth (Matteini et al., 2009). This indicates the disruption of intermolecular interactions at high temperature which was further supported by differential scanning calorimetry (DSC) and FTIR

within the same study. These observations are coherent with our calculations of the strength of the interchain interaction which moderately decreases with the growing temperature, as indicated by the mean distance of the chains (Fig. 3) and the frequency of interactions (Fig. S11). A similar effect was observed in a recent study of approx. 2 MDa HA in solutions of various salts (Musilová, Kaspárková, Mráček, Minarík, & Minarík, 2019). In the 0.1 M solutions of different salts, especially NH_4SCN and Na_2SO_4 , a sudden break of the temperature dependence of the hydrodynamic radius can be observed at a temperature specific for each salt. We can thus speculate that this phenomenon is caused by the sudden decrease of the number of interactions between the chains at the given temperature resulting in the decay of the organized structure of the coil. For NaCl , however, only a small change of the trend was observed by those authors which agrees with the weak temperature dependence of the number of intermolecular interactions observed in our calculations. An interesting study of dense HA brushes (Chen & Richter, 2019) shows that the HA chains forming this brush adopt a stretched conformation at the salt-free solution indicating again the impossibility of interchain interactions when ions are absent. The subsequent decrease of the brush thickness with the growing salt concentration can be attributed to both the effect of the salt on a single chain and the intramolecular interactions. Although the thickness decreases more rapidly than the radius of gyration of a single random coil (Sorci & Reed, 2004), the evaluation of the contributions of these two phenomena is difficult due to the different chain conformations and the local environment of the chains, therefore it would require genuine simulations of the brush. The disproportionately strong effect of Ca^{2+} cations compared to their ion strength shown in the same study indicates the enhanced formation of salt bridges with the bivalent cations. A similar phenomenon was observed by (Innes-Gold, Pincus, Stevens, & Saleh, 2019) for trivalent cations. Thus, in the presence of multiply charged cations able to balance or overbalance the negative charge of two carboxylate groups the salt bridges may cause strong interaction between the HA chains, while with the monovalent cations this effect is very weak.

The electrostatic repulsion between the HA chains can also be reduced by low pH at which the carboxylic groups are mostly protonated, as shown by our calculations with fully protonated HA in an artificial solvent not interacting electrostatically with the HA chains. Experimental studies (Giubertoni, Burla, et al., 2019; Giubertoni, Burla, Bakker, & Koenderink, 2020) showed that interactions among the HA chains in real solution can lead even to gel formation in a certain range of low pH. The identified hydrogen bonds between the amide and carboxyl group can be formed only when substantial part of the carboxyl groups are protonated which is a probable reason of their absence in our simulation with all these groups dissociated. MD simulations of HA chains with different protonization states of the carboxyl groups could help us to understand this interesting phenomenon in deeper detail and may become an inspiration of our future research.

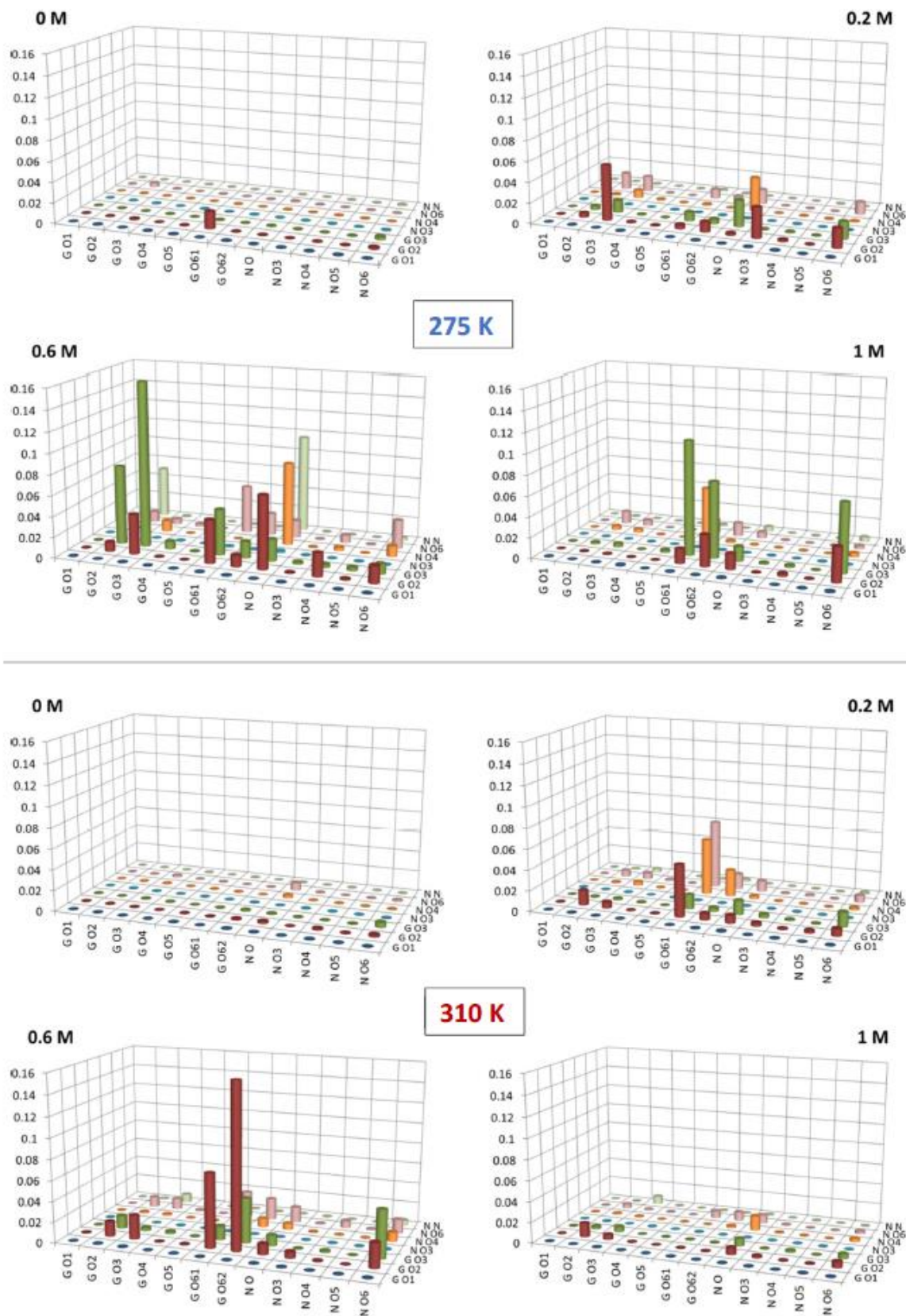


Fig. 8. Frequency of intermolecular hydrogen bonds per a simulation frame between individual donor (right axis) and acceptor (front axis) groups for two temperatures and four NaCl concentrations.

5. Conclusions

Hyaluronan molecules have a natural tendency to form duplex double-helical structures. However, their existence is possible only in strongly non-polar environments simulated in our study by solvent interacting with HA molecules only by dispersion forces. Therefore, existence of these structures cannot be excluded in non-polar solvents or in crystals as shown by some previous papers. In aqueous solution, on the contrary, no stable duplex structures are viable due to the intensive solvation of each HA chain individually. In pure water the electrostatic repulsion completely disables the approach of two chains which results in a negligible number of contacts between them. However, the increase of NaCl concentration increases the tendency to form temporary duplex structures as the dissolved ions associate with HA chains and decrease their negative charge allowing them to approach one another. This opens the way for the constitution of the duplex-stabilizing intermolecular hydrogen bonds. On the contrary, the salt concentration generally reduces the ability to form hydrogen bonds. These two counteracting phenomena result to a maximum intensity of the HA-HA interaction at the NaCl concentration of 0.6 M. Although the intermolecular binding is relatively weak and incapable of stabilizing permanent duplex structures, it may influence the behavior of HA in highly concentrated solutions above 10 mg/ml or in large HA macromolecules as evidenced by various experimental data. Thus, this study is the first attempt to analyze the interaction between two HA chains and its tendency to form duplex structures. In spite of its weakness at the selected conditions, clear trends are observed that are in accord with published experiments. Hence, combining experiments with MD simulations may provide a deeper insight even in complex HA systems with strong application potential like gels, nanoparticles or molecular brushes.

References

- Almond, A., Deangelis, P. L., & Blundell, C. D. (2006). Hyaluronan: The local solution conformation determined by NMR and computer modeling is close to a contracted left-handed 4-fold helix. *Journal of Molecular Biology*, 358(5), 1256-1269. <https://doi.org/10.1016/j.jmb.2006.02.077>
- Arnott, S., Mitra, A. K., & Raghunathan, S. (1983). Hyaluronic acid double helix. *Journal of Molecular Biology*, 169(4), 861-872. [https://doi.org/10.1016/S0022-2836\(83\)80140-5](https://doi.org/10.1016/S0022-2836(83)80140-5)
- Bełdowski, P., Mazurkiewicz, A., Topolmski, T., & Małek, T. (2019). Hydrogen and water bonding between glycosaminoglycans and phospholipids in the synovial fluid: Molecular dynamics study. *Materials*, 12(13), 2060. <https://doi.org/10.3390/ma12132060>
- Blundell, C. D., DeAngelis, P. L., & Almond, A. (2006). Hyaluronan: The absence of amide-carboxylate hydrogen bonds and the chain conformation in aqueous solution are incompatible with stable secondary and tertiary structure models. *Biochemical Journal*, 396(3), 487-498. <https://doi.org/10.1042/BJ20060085>
- Chen, X., & Richter, R. P. (2019). Effect of calcium ions and pH on the morphology and mechanical properties of hyaluronan brushes. *Interface Focus*, 9(2), 20180061. <https://doi.org/10.1098/rsfs.2018.0061>
- Cox, W. P., & Merz, E. H. (1958). Correlation of dynamic and steady flow viscosities. *Journal of Polymer Science*, 28(118), 619-622. <https://doi.org/10.1002/pol.1958.1202811812>

Dea, I. C. M., Moorhouse, R., Rees, D. A., Arnott, S., Guss, J. M., & Balazs, E. A. (1973). Hyaluronic acid: A novel, double helical molecule. *Science*, 179(4073), 560-562. <https://doi.org/10.1126/science.179.4073.560>

Donati, A., Magnani, A., Bonechi, C., Barbucci, R., & Rossi, C. (2001). Solution structure of hyaluronic acid oligomers by experimental and theoretical NMR, and molecular dynamics simulation. *Biopolymers*, 59(6), 434-445. [https://doi.org/10.1002/1097-0282\(200111\)59:6<434::AID-BIP1048>3.0.CO;2-4](https://doi.org/10.1002/1097-0282(200111)59:6<434::AID-BIP1048>3.0.CO;2-4)

Fischer, E., Callaghan, P. T., Heatley, F., & Scott, J. E. (2002). Shear flow affects secondary and tertiary structures in hyaluronan solution as shown by rheo-NMR. *Journal of Molecular Structure*, 602-603, 303-311. [https://doi.org/10.1016/S0022-2860\(01\)00733-5](https://doi.org/10.1016/S0022-2860(01)00733-5)

Fouissac, E., Milas, M., Rinaudo, M., & Borsali, R. (1992). Influence of the ionic strength on the dimensions of sodium hyaluronate. *Macromolecules*, 25(21), 5613-5617. <https://doi.org/10.1021/ma00047a009>

Furlan, S., La Penna, G., Perico, A., & Cesaro, A. (2005). Hyaluronan chain conformation and dynamics. *Carbohydrate Research*, 340(5), 959-970. <https://doi.org/10.1016/j.carres.2005.01.030>

Giubertoni, G., Burla, F., Bakker, H. J., & Koenderink, G. H. (2020). Connecting the stimuli-responsive rheology of biopolymer hydrogels to underlying hydrogenbonding interactions. *Macromolecules*, 53(23), 10503-10513. <https://doi.org/10.1021/acs.macromol.0c01742>

Giubertoni, G., Burla, F., Martinez-Torres, C., Dutta, B., Pletikapic, G., Pelan, E.,

Rezus, Y. L. A., Koenderink, G. H., & Bakker, H. J. (2019). Molecular origin of the elastic state of aqueous hyaluronic acid. *The Journal of Physical Chemistry B*, 123(14), 3043-3049. <https://doi.org/10.1021/acs.jpcc.9b00982>

Giubertoni, G., Koenderink, G. H., & Bakker, H. J. (2019). Direct observation of intrachain hydrogen bonds in aqueous hyaluronan. *The Journal of Physical Chemistry A*, 123(38), 8220-8225. <https://doi.org/10.1021/acs.jpca.9b06462>

Gibbon, P., Heng, B. C., & Hardingham, T. E. (2000). The analysis of intermolecular interactions in concentrated hyaluronan solutions suggest no evidence for chain-chain association. *Biochemical Journal*, 350(Pt 1), 329-335.

Guench, O., Hatcher, E., Venable, R. M., Pastor, R. W., & MacKerell, A. D. (2009). CHARMM additive all-atom force field for glycosidic linkages between hexopyranoses. *Journal of Chemical Theory and Computation*, 5(9), 2353-2370. <https://doi.org/10.1021/ct900242e>

Hansen, H. S., & Hunenberger, P. H. (2011). A reoptimized GROMOS force field for hexopyranose-based carbohydrates accounting for the relative free energies of ring conformers, anomers, epimers, hydroxymethyl rotamers, and glycosidic linkage conformers. *Journal of Computational Chemistry*, 32(6), 998-1032. <https://doi.org/10.1002/jcc.21675>

Hayashi, K., Tsutsumi, K., Nakajima, F., Norisuye, T., & Teramoto, A. (1995). Chain-stiffness and excluded-volume effects in solutions of sodium hyaluronate at high ionic strength. *Macromolecules*, 28(11), 3824-3830. <https://doi.org/10.1021/ma00115a012>

Holmbeck, S. M., Petillo, P. A., & Lerner, L. E. (1994). The solution conformation of hyaluronan: A combined NMR and molecular dynamics study. *Biochemistry*, 33(47), 14246-14255.

Humphrey, W., Dalke, A., & Schulten, K. (1996). VMD: Visual molecular dynamics. *Journal of Molecular Graphics*, 14(1), 27-28. [https://doi.org/10.1016/0263-7855\(96\)00018-5](https://doi.org/10.1016/0263-7855(96)00018-5), 33-38.

Ingr, M., Kutáľková, E., & Hrnčířík, J. (2017). Hyaluronan random coils in electrolyte solutions—a molecular dynamics study. *Carbohydrate Polymers*, 170, 289-295. <https://doi.org/10.1016/j.carbpol.2017.04.054>

Innes-Gold, S. N., Pincus, P. A., Stevens, M. J., & Saleh, O. A. (2019). Polyelectrolyte conformation controlled by a trivalent-rich ion jacket. *Physical Review Letters*, 123 (18), Article 187801. <https://doi.org/10.1103/PhysRevLett.123.187801>

Krieger, E., & Vriend, G. (2014). YASARA View—Molecular graphics for all devices—From smartphones to workstations. *Bioinformatics (Oxford, England)*, 30 (20), 2981-2982. <https://doi.org/10.1093/bioinformatics/btu426>

Kutalkova, E., Hrnčířík, J., Witasek, R., & Ingr, M. (2020). Effect of solvent and ions on the structure and dynamics of a hyaluronan molecule. *Carbohydrate Polymers*, 234, Article 115919. <https://doi.org/10.1016/j.carbpol.2020.115919>

Leibler, L., Rubinstein, M., & Colby, R. H. (1991). Dynamics of reversible networks.

Macromolecules, 24(16), 4701-4707. <https://doi.org/10.1021/ma00016a034> Matteini, P., Dei, L., Carretti, E., Volpi, N., Goti, A., & Pini, R. (2009). Structural behavior of highly concentrated hyaluronan. *Biomacromolecules*, 10(6), 1516-1522. <https://doi.org/10.1021/bm900108z>

Mendichi, R., Solteás, L., & Giacometti Schieron, A. (2003). Evaluation of radius of gyration and intrinsic viscosity molar mass dependence and stiffness of hyaluronan. *Biomacromolecules*, 4(6), 1805-1810. <https://doi.org/10.1021/bm0342178>

Michaud-Agrawal, N., Denning, E. J., Woolf, T. B., & Beckstein, O. (2011). MDAAnalysis: A toolkit for the analysis of molecular dynamics simulations. *Journal of Computational Chemistry*, 32(10), 2319-2327. <https://doi.org/10.1002/jcc.21787>

Musilová, L., Kaspářková, V., Mráček, A., Minářík, A., & Minářík, M. (2019). The behaviour of hyaluronan solutions in the presence of Hofmeister ions: A light scattering, viscometry and surface tension study. *Carbohydrate Polymers*, 212, 395-402. <https://doi.org/10.1016/j.carbpol.2019.02.032>

Payne, W. M., Svehkarev, D., Kyrchenko, A., & Mohs, A. M. (2018). The role of hydrophobic modification on hyaluronic acid dynamics and self-assembly. *Carbohydrate Polymers*, 182, 132-141. <https://doi.org/10.1016/j.carbpol.2017.10.054>

Phillips, J. C., Braun, R., Wang, W., Gumbart, J., Tajkhorshid, E., Villa, E., Chipot, C., Skeel, R. D., Kaleá, L., & Schulten, K. (2005). Scalable molecular dynamics with NAMD. *Journal of Computational Chemistry*, 26(16), 1781-1802. <https://doi.org/10.1002/jcc.20289>

Samantray, S., Olubiyi, O. O., & Strodel, B. (2021). The influences of sulphation, salt type, and salt concentration on the structural heterogeneity of glycosaminoglycans.

International Journal of Molecular Sciences, 22(21), 11529. <https://doi.org/10.3390/ijms222111529>

Scott, J. E., & Heatley, F. (1999). Hyaluronan forms specific stable tertiary structures in aqueous solution: A ¹³C NMR study. *Proceedings of the National Academy of Sciences*, 96(9), 4850-4855. <https://doi.org/10.1073/pnas.96.9.4850>

Scott, J. E., & Heatley, F. (2002). Biological properties of hyaluronan in aqueous solution are controlled and sequestered by reversible tertiary structures, defined by NMR spectroscopy. *Biomacromolecules*, 3(3), 547-553. <https://doi.org/10.1021/bm010170j>

Sheehan, J. K., Gardner, K. H., & Atkins, E. D. T. (1977). Hyaluronic acid: A doublehelical structure in the presence of potassium at low pH and found also with the cations ammonium, rubidium and caesium. *Journal of Molecular Biology*, 117(1), 113-135. [https://doi.org/10.1016/0022-2836\(77\)90027-4](https://doi.org/10.1016/0022-2836(77)90027-4)

Siódmiak, J., Bełdowski, P., Auge, W. K., Ledziński, D., Smigiel, S., & Gadomski, A. (2017). Molecular dynamic analysis of hyaluronic acid and phospholipid interaction in tribological surgical adjuvant design for osteoarthritis. *Molecules (Basel, Switzerland)*, 22(9). <https://doi.org/10.3390/molecules22091436>

Smith, P., Ziolek, R. M., Gazzarrini, E., Owen, D. M., & Lorenz, C. D. (2019). On the interaction of hyaluronic acid with synovial fluid lipid membranes. *Physical Chemistry Chemical Physics*, 21(19), 9845-9857. <https://doi.org/10.1039/C9CP01532A>

Sorci, G. A., & Reed, W. F. (2004). Effect of valence and chemical species of added electrolyte on polyelectrolyte conformations and interactions. *Macromolecules*, 37 (2), 554-565. <https://doi.org/10.1021/ma035551z>

Staskus, P. W., & Johnson, W. C. (1988a). Conformational transition of hyaluronic acid in aqueous-organic solvent monitored by vacuum ultraviolet circular dichroism. *Biochemistry*, 27(5), 1522-1527. <https://doi.org/10.1021/bi00405a019>

Staskus, P. W., & Johnson, W. C. (1988b). Double-stranded structure for hyaluronic acid in ethanol-aqueous solution as revealed by circular dichroism of oligomers. *Biochemistry*, 27(5), 1528-1534. <https://doi.org/10.1021/bi00405a020>

Van Der Spoel, D., Lindahl, E., Hess, B., Groenhof, G., Mark, A. E., & Berendsen, H. J. C. (2005). GROMACS: Fast, flexible, and free. *Journal of Computational Chemistry*, 26 (16), 1701-1718. <https://doi.org/10.1002/jcc.20291>

Yaffe, N. R., Almond, A., & Blanch, E. W. (2010). A new route to carbohydrate secondary and tertiary structure using raman spectroscopy and Raman optical activity. *Journal of the American Chemical Society*, 132(31), 10654-10655. <https://doi.org/10.1021/ja104077n>

Yu, F., Zhang, F., Luan, T., Zhang, Z., & Zhang, H. (2014). Rheological studies of hyaluronan solutions based on the scaling law and constitutive models. *Polymer*, 55 (1), 295-301. <https://doi.org/10.10Wj.polymer.2013.11.047>